

Epidemic Spreading and Digital Contact Tracing: Effects of Heterogeneous Mixing and Quarantine Failures

Abbas K. Rizi,¹ Ali Faqeeh,^{1,2,3} Arash Badie-Modiri,¹ and Mikko Kivelä¹

¹*Department of Computer Science, School of Science, Aalto University, FI-0007, Finland*

²*Mathematics Applications Consortium for Science & Industry, University of Limerick, Ireland*

³*CNetS, School of Informatics, Computing, & Engineering, Indiana University, Bloomington, IN, USA*

(Dated: March 1, 2025)

Contact tracing via digital tracking applications installed on mobile phones is an important tool for controlling epidemic spreading. Its effectivity can be quantified by modifying the standard methodology for analyzing percolation and connectivity of contact networks. We apply this framework to networks with varying degree distributions, numbers of application users, and probabilities of quarantine failures. Further, we study structured populations with homophily and heterophily and the possibility of degree-targeted application distribution. Our results are based on a combination of explicit simulations and mean-field analysis. They indicate that there can be major differences in the epidemic size and epidemic probabilities which are equivalent in the normal SIR processes. Further, degree heterogeneity is seen to be especially important for the epidemic threshold but not as much for the epidemic size. The probability that tracing leads to quarantines is not as important as the application adoption rate. Finally, both strong homophily and especially heterophily with regard to application adoption can be detrimental. Overall, epidemic dynamics are very sensitive to all of the parameter values we tested out, which makes the problem of estimating the effect of digital contact tracing an inherently multidimensional problem.

Until effective vaccines are widely deployed in a pandemic era, carefully timed non-pharmaceutical interventions [1] such as wearing face masks [2], school closures, travel restrictions and contact tracing [3–7] are the best tools we have for curbing the pandemic. Contact tracing is an attempt to discover and isolate asymptomatic or pre-symptomatic (exposed) individuals. In the absence of herd immunity, contact tracing is a potent low-cost intervention method since it puts people into quarantine where and when the disease spreads. Therefore, it can have a significant role in containing a pandemic by relaxing social-distancing interventions [8], providing an acceptable trade-off between public health and economic objectives [9, 10], developing sustainable exit strategies [11, 12], identifying future outbreaks [13], and reaching the ‘source’ of infection [14].

Thanks to the emergence of low-cost wearable health devices [15–21] and mobile software applications, digital contact tracing can now be deployed with higher precision without the problems of manual contact tracing, such as the tracing being slow and labor-intensive or people’s hesitation to give identifying data about their contacts due to blame, fear, confusion, or politics. On the other hand, smartphones and wearable devices also offer continuous access to real-time physiological data which can be used to tune other non-pharmaceutical or pharmaceutical strategies. Modern apps enable us to monitor COVID-19 symptoms [22–24], identify its hotspots [25], track mosquito-borne diseases such as Malaria, Zika and Dengue [26, 27], and detect microscopic pathogens.

In both forms—manual [4, 5, 28–36] and digital [37–40]—contact tracing has been commonly considered as an effective strategy and different empirical data sets have validated this claim in short-time population-based controlled experiments [37, 41–45]. It has been estimated

that for every percentage point increase in app-users, the number of cases can be reduced by 2.3% (in statistical analysis) [46]. However, the real potential of contact tracing in heterogeneous populations [47–50] is not as clear, mainly because of the homophily in app adoption and other health behavior [51, 52]. It has been reported that app adoption is correlated with people’s jobs, age, income and nationality [53, 54]. In addition, degree-heterogeneity in the contact network [55] can alter epidemiological properties in the form of variance in final outbreak size [56], vanishing epidemic threshold [50, 57], hierarchical spreading [58], strong finite-size effects [59] and universality classes for critical exponents [60].

The fraction of population that adopts the app is not the only important factor for reducing the peak and total size of the epidemic, but also the distribution and timing of contact tracing is of great significance. Therefore, in some parameter settings, contact tracing may not be effective enough [8, 61, 62]. App adoption of super-spreaders [63, 64] is needed to be taken into account to curb the epidemic since it dictates the extent to which a virus spreads in a bursty fashion [65–67], especially when there is high individual-level variation in the number of secondary transmissions [58, 68, 69].

Since the World Health Organization has declared the COVID-19 outbreak as a Public Health Emergency of International Concern, network scientists have developed different approaches towards analyzing epidemic tracing and mitigation with apps. Using the toolbox of network science, different groups have investigated the effectiveness of contact tracing based on the topology and directionality of contact networks [14, 41, 70–76]. Recently, a mathematical framework aimed at understanding how homophily in health behavior shapes the dynamics of epidemics has been introduced by Burgio *et al.* [77]. This

study expanded the model of Bianconi et al. [70] and computed the reproduction number and attack rate in a homophilic populations using mean-field equations.

Our study investigates the effect of varying app coverage on the epidemic's threshold, probability and expected size in homogeneous and heterogeneous contact networks with and without homophily or heterophily in app adoption. Further, we explore the effect of distributing the apps randomly and preferentially to high-degree nodes [70] in these scenarios. Our main focus is on the epidemic threshold and the final size of the epidemics. Therefore, we assume the dynamics of the epidemic to be governed by the simple SIR model [55]. This model can be easily mapped to a static bond-percolation problem [78, 79] so that the epidemiological properties can be measured based on the topological structure of the underlying network [55, 80–83]. The difference in the spreading framework with the app to the normal one is that the infection cannot spread further if it passes a link between two app-users (app-adopters). That is, the infection process model needs to include the memory of the type of node it is coming from. We then extend the percolation framework such that we can add memory [84, 85] to it in order to keep track of the infection path. This leads to the observation that the epidemic size is not the same as the epidemic probability anymore.

Our results are largely based on mean-field-type calculations of the percolation problem, which are confirmed by explicit simulations of SIR epidemic process and measurements of component sizes in finite networks. Our findings show that: 1) the number of app-users has a direct effect on the epidemic size and epidemic probability and the difference between these two observables is larger in high-degree targeting strategy; 2) epidemics can be controlled to a much better degree in the high-degree targeting strategy; 3) even though degree-heterogeneity can strongly affect or even eliminate the epidemic threshold, high-degree targeting strategy can compensate this effect and increase the threshold significantly; 4) increasing heterophily from random mixing always increases the outbreak size and lowers the epidemic threshold; 5) increasing homophily does the opposite until an optimum, that is below the maximum homophily case, is reached; and finally 6) the probability of contact tracing succeeding in preventing further infections is not as crucial as the fraction of app-users, but can still have significant effects on the epidemic size and epidemic threshold. The only exception is when the apps are distributed to heterogeneous networks with the high-degree targeting strategy.

I. MODELLING APPROACH

A. Disease model and connection to percolation

We employ a standard SIR disease model on networks with additional dynamics given by the disease interactions in the presence of the disease tracking application.

In the model an infected (I) node will infect susceptible (S) nodes it is connected to by rate β and go to the removed state (R) after time τ . In addition, if an app-user infects another app-user, that second node will get infected but will quarantine themselves with probability p_{app} . The quarantined user will have no further connections that would spread the infection they received from the other app-user. A substantial deviation from a realistic spreading case in our model is that the quarantine does not prevent the disease spreading to the quarantined node through a third node. That is, we only model the primary infection path from the other app-user causing the alarm but do not stop possible concurrent secondary infection paths from a third node.

The SIR processes can be studied using component size distributions of networks where parts of the links are randomly removed. The SIR spreading process can be mapped to a slightly more complicated percolation problem in the presence of apps [41, 70]. Thus, the epidemic threshold, epidemic probability and epidemic size can be read from percolation simulations [78, 86, 87]. In this mapping, every infected individual, regardless of app adoption, can infect a susceptible neighbor with transmission probability $p = 1 - e^{-\beta\tau}$ [78]. Moreover, to model app-user quarantines, one needs to delete the links between two app-users with the probability of successful quarantine due to the app, p_{app} . This ensures that we ignore the infection paths through two app-users when one of them is successfully quarantined. However, removing these links also removes the second app-user from the component, even though they are infected. To correct this, we need first to find the network components and then extend them by including all app-users outside of the component connected to another app-user (and considering the probability p that the link is kept). See Fig. 1 for an illustration of this process, which leads us to two definitions of components: normal and extended.

B. Components, epidemic size and epidemic probability

In the SIR model without apps, the component size distribution can be used to approximately describe the late stages of the epidemics. Given an initially infected node, the size of the component it belongs to determines the size of the epidemic. The relationship between percolation and the final epidemic size is straightforward if the population is large enough that it can be approximated with an infinite contact network. In this case, the percolation threshold gives the epidemic threshold and below it, the epidemic always spans only a zero fraction of the population because all the components are of finite size. Above the percolation threshold, there is a single giant component that spans $s_{\text{max}} = S_{\text{max}}/N$ fraction of the nodes. This is equivalent to both the size of the epidemic, given that there is one, and the probability that there is an epidemic starting from a single initially in-

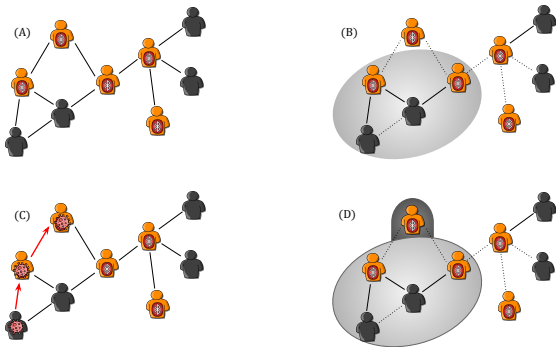


FIG. 1. (a) Original contact network with app-users marked with the oval symbol. (b) The normal largest component, after the dotted links have been removed in the percolation process by random. When apps are working perfectly, links between a pair of app-users are removed with probability $p_{\text{app}} = 1$ and other links are removed with probability p . (c) An example for a path of infection: the second app-user can be infected; therefore it must be included in the outbreak size (d) Extending the giant component to include the secondary app infections. The second infected app-adaptor is added to the giant component with transmission probability p .

ected node [78]. The expected epidemics size in fraction of eventually infected nodes is in this case given as s_{max}^2 .

When we introduce apps to the spreading process, the equivalence of the epidemic size and epidemic probability breaks down. Both the normal component and the extended component become important. The component size still gives the probability that there is an epidemic as in the normal SIR process. However, the epidemic size, given that there is one, is now given by the extended component size s'_{max} . The expected epidemic size is then given by $s_{\text{max}} s'_{\text{max}}$.

Similar relationships hold for finite-size systems. For example, the expected size of the epidemics from single source becomes

$$\langle E \rangle = \sum_c \frac{S_c}{N} S'_c, \quad (1)$$

where S_c is the normal size and S'_c is the extended size of the component c and N is the total number of nodes. In this formula, S_c/N gives the probability that the initially infected node is in the component c and S'_c gives the size of the epidemic if a node in component c is chosen.

C. Network models

We aim to study how the network topology and the app-users' locations affect the epidemics. We study networks with degree distribution $P(k)$ and average degree $\langle k \rangle$ such that each node is an app-user with probability π_a and not an app-user with probability $1 - \pi_a$. We use Poisson (ER) random graphs [88] to model homogeneous contact patterns and scale-free networks generated with

the configuration model [55] where $P(k) \propto k^{-3}$ to model heterogeneous contact patterns. The $\pi_a N$ app-users can be picked 1) uniformly at random from the underlying network or 2) by distributing the apps in the order of their degree such that the high-degree nodes get the apps first.

To insert homophily (heterophily) in app adoption, we assume that app-users are more likely (are less likely) to be connected together. This can be controlled by the probability π_{aa} that an app-user is connected to another app-user; this stochastic block model network is a type of $E^{i,i'}$ network introduced in Ref [89] with two groups of nodes: app-users and individuals without the app. The existence of homophily or heterophily of the network structure is determined by comparing π_{aa} to its value for the neutral case with no homophily or heterophily.

In the absence of homophily or heterophily, $\pi_{aa} = \eta_a$, where η_a is the ratio of links that emerge from app-users to the total number of stubs (nodes connections); this is because if the nodes were connected purely at random, the probability that a link from an app-user connects it to another app-user equals the ratio of the number of stubs that app-users have to the total number of stubs, i.e., η_a . In the case of a random selection of app-users $\eta_a = \pi_a$, since both app-users and non-app-users have on average the same number of stubs and the fraction of stubs that app-users have equals the fraction of app-users in the system, i.e., π_a . Nonetheless, in a high-degree targeting strategy, the number of stubs that app-users have on average is larger than that of non-app-users. In that case, η_a can be calculated from the degree distribution (see Sec. II A). When $\pi_{aa} > \eta_a$, app-users are more likely to be connected to each other than a purely random network in which they are connected with probability η_a . Hence, there is homophily in the connection between the app-users, which means there is also homophily in the connections between non-app-users. On the other hand, when $\pi_{aa} < \eta_a$ nodes are more likely to be connected to the nodes of the other type (heterophilic network).

II. ANALYTIC AND SIMULATION METHODS

The epidemics are studied here with various methods of approximation. We employ analytical computations based on mean-field-type approximations to efficiently analyze our models' wide parameter space and provide explicit formulas for our main observable quantities. Here an approximation based on branching processes can be used to determine the critical point. Following Ref. [41], a more detailed calculation based on percolation arguments will give us the component sizes which can be related to the final epidemic size and epidemic probability. Simulations of the network connectivity then complement these mean-field approximations. Finally, we explore the accuracy of the mean-field approximations via explicit simulations of the SIR model.

A. Giant component size from consistency equations

To study the behavior of the epidemic dynamics, we form consistency equations for the giant component size. In Ref. [41] the governing equations for the size of the epidemic and the transition point were obtained for the case of random networks in the absence of homophily. Here we derive the analytical results for the more general case of the spectrum of heterophilic to homophilic networks of Ref. [41]. We consider that app-users might be connected together with a pattern different from pure random chance. This can also be the case for the non-app-users. In a homophilic network, app/non-app-users are more likely to connect to individuals of the same kind. This is equivalent to saying that groups of people who adopted the app are likely to be groups of nodes in the network with members at a relatively close distance from each other. To represent the bias in connection probabilities we consider that a link from an app-user is connected to another app-user with probability π_{aa} and other types of links were formed with probabilities $\pi_{an} = 1 - \pi_{aa}$, $\pi_{na} = \frac{\pi_a}{1 - \pi_a}(1 - \pi_{aa})$ and $\pi_{nn} = 1 - \pi_{na} = \frac{1 - \pi_a - \pi_a(1 - \pi_{aa})}{1 - \pi_a}$, where π_a is the probability that a person is an app-user and the second equality comes from the balance between the number of links from app-users to non-app-users and from non-app to app-users, that is, $\pi_a N \pi_{an} \langle k \rangle = (1 - \pi_a) N \pi_{na} \langle k \rangle$.

We aim to write the self-consistency equations for the probability, u_0 , that following a link to a non-app-user does not lead to the giant component and probability u_a , that following a link to an app-user does not lead to the giant component. Using these probabilities, the relative size of the giant component s and the relative size of the extended giant component s' can be obtained, where s is, in fact, the fraction of nodes infected through non-app-users, while s' also includes individuals caught infection though an app-user before s/he could quarantine her/himself (see Sec. II C 1).

Similar to Ref. [41], we can write the conditional probabilities of u_0 and u_a given that they have degree k as

$$u_0(k) = \sum_{k'=0}^k \binom{k}{k'} \pi_{na}^{k'} u_a^{k'} (1 - \pi_{na})^{k-k'} u_0^{k-k'}, \quad (2)$$

$$u_a(k) = \sum_{k'=0}^k \binom{k}{k'} \pi_{aa}^{k'} (1 - \pi_{aa})^{k-k'} u_0^{k-k'}. \quad (3)$$

Then using a treatment similar to Ref. [41], the self-consistency equations can be written as:

$$u_0 = g_1((1 - \pi_{na})u_0 + \pi_{na}u_a), \quad (4)$$

$$u_a = g_1((1 - \pi_{aa})u_0 + \pi_{aa}(p_{app} + (1 - p_{app})u_a)), \quad (5)$$

and

$$s = 1 - (1 - \pi_a)g_0((1 - \pi_{na})u_0 + \pi_{na}u_a) - \pi_a g_0((1 - \pi_{aa})u_0 + \pi_{aa}(p_{app} + (1 - p_{app})u_a)), \quad (6)$$

where g_0 and g_1 are, respectively, the generating functions for degree and extended degree distributions [55], p_{app} is the probability the apps work as expected. $1 - p_{app}$ is then the probability that the app-user does not quarantine her/himself after being notified of an exposure by an infectious app-user. Note that π_{na} is determined by the free parameters π_a and π_{aa} as we already showed that $\pi_{na} = \frac{\pi_a}{1 - \pi_a}(1 - \pi_{aa})$.

We can approximate s' by writing:

$$s' = 1 - (1 - \pi_a)g_0((1 - \pi_{na})u_0 + \pi_{na}u_a) - \pi_a g_0((1 - \pi_{aa})u_0 + \pi_{aa}u_a), \quad (7)$$

where, as opposed to Eq. 6, the third term is not a function of p_{app} and the reason is that Eq. 6 assumes that if the app works (which happens with probability p_{app}) then the probability that a link connected to an app-user does not lead to the giant component is 1 (while if the app does not work it is u_a). However, whether the app works or not, the probability that an app-user does not get infected from another app-user is u_a . When apps work, if the second app-user is infected, she quarantines herself and does not infect any other node).

In the case of including a transmission probability p which is less than 1 (in the above equations it was assumed the links are transmitting with probability 1), Eqs. 4 and 5 will change to:

$$u_0 = 1 - p + pg_1((1 - \pi_{na})u_0 + \pi_{na}u_a), \quad (8)$$

$$u_a = 1 - p + pg_1((1 - \pi_{aa})u_0 + \pi_{aa}(p_{app} + (1 - p_{app})u_a)). \quad (9)$$

When the fraction π_a of nodes selected to adopt the app are all the highest degree nodes in the network, these nodes all have a degree higher than $k_a - 1$ such that they include some of k_a nodes and the rest are comprised of all nodes with degree larger than k_a . Then for the fraction η_a of the links protruding from the app-users (which are the top π_a fraction of nodes) can write:

$$\eta_a = r^* k_a p_{k_a} / \langle k \rangle + \sum_{k_a+1}^{\infty} k p_k / \langle k \rangle \quad (10)$$

$$= \sum_{k_{a, \text{right}}}^{\infty} k p_k / \langle k \rangle, \quad (11)$$

where r^* is the fraction of degree k_a nodes that are app-users and in Eq. 11 we absorbed r^* into p_k so that $p_{k_{a, \text{right}}} = r^* p_{k_a}$ represents the fraction of nodes in the network that have degree k_a and are app-users (so in Eq. 11, $k_{a, \text{right}}$ takes the value k_a).

Then for a network with homo/heterophily:

$$u_0 = 1 - p + p \frac{1}{1 - \eta_a} \sum_{k=0}^{k_{a,\text{left}}} q_k [(1 - \pi_{na})u_0 + \pi_{na}u_a]^k, \quad (12)$$

$$u_a = 1 - p + p \frac{1}{\eta_a} \sum_{k_{a,\text{right}}}^{\infty} q_k [(1 - \pi_{aa})u_0 + \pi_{aa}(p_{\text{app}} + (1 - p_{\text{app}})u_a)]^k, \quad (13)$$

and

$$s = 1 - \sum_{k=0}^{k_{a,\text{left}}} p_k [(1 - \pi_{na})u_0 + \pi_{na}u_a]^k - \sum_{k_{a,\text{right}}}^{\infty} p_k [(1 - \pi_{aa})u_0 + \pi_{aa}(p_{\text{app}} + (1 - p_{\text{app}})u_a)]^k. \quad (14)$$

A special case of which are networks with neutral (non-existing) homophily, where π_{aa} is obtained to be equal to η_a and accordingly $\pi_{na} = \eta_a$, therefore,

$$u_0 = 1 - p + p \frac{1}{1 - \eta_a} \sum_{k=0}^{k_{a,\text{left}}} q_k [(1 - \eta_a)u_0 + \eta_a u_a]^k \quad (15)$$

$$u_a = 1 - p + p \frac{1}{\eta_a} \sum_{k_{a,\text{right}}}^{\infty} q_k [\eta_a(p_{\text{app}} + (1 - p_{\text{app}})u_a) + (1 - \eta_a)u_0]^k, \quad (16)$$

and

$$s = 1 - \sum_{k=0}^{k_{a,\text{left}}} p_k [(1 - \eta_a)u_0 + \eta_a u_a]^k - \sum_{k_{a,\text{right}}}^{\infty} p_k [\eta_a(p_{\text{app}} + (1 - p_{\text{app}})u_a) + (1 - \eta_a)u_0]^k. \quad (17)$$

These results predict the behavior of the epidemic dynamics in the thermodynamic limit. Therefore they describe the dynamics very well when the network size is large enough.

B. Mean-field approximation for the branching process

An alternative to writing the consistency equations for the giant component size is to assume that a branching process governs the epidemic dynamics. Then, a straightforward way of finding the epidemic threshold in the SIR model is to find the critical point of a branching process, where the branching factor is given by the expected excess degree q . In the epidemic setting, the branching factor $\bar{k} = pq$ gives the expected number of people one

infected person infects during the epidemic process. Note that this is different from the basic reproduction number which has been defined in the networks as $R_0 = \beta/\gamma \langle k \rangle$ [79]. In the SIR model with the app, we need to duplicate the populations so that we separately track the ones without the app (S_n , I_n and R_n) and with the app (S_a , I_a and R_a).

Given that the apps are uniformly distributed to π_a fraction of the nodes and \bar{k} is the branching factor, we can write a mean-field approximation based on the branching process as follows:

$$I_n^{(t+1)} = \bar{k} (\pi_{nn} I_n^{(t)} + \pi_{an} I_a^{(t)}), \quad (18)$$

$$I_a^{(t+1)} = \bar{k} (\pi_{na} I_n^{(t)} + \pi_{aa} (1 - p_{\text{app}}) I_a^{(t)}). \quad (19)$$

By defining $a = \pi_{nn} \bar{k}$, $b = \pi_{na} \bar{k}$, $c = \pi_{an} \bar{k}$ and $d = \pi_{aa} \bar{k} (1 - p_{\text{app}})$, the difference equations can be written as:

$$\mathbf{X}_{t+1} = \mathbf{A} \mathbf{X}_t, \quad (20)$$

where $\mathbf{X}_t = \begin{pmatrix} I_n^{(t)} \\ I_a^{(t)} \end{pmatrix}$ and $\mathbf{A} = \begin{pmatrix} a & b \\ c & d \end{pmatrix}$.

The steady state $\mathbf{X}_{t+1} = \mathbf{X}_t$ is possible if all the eigenvalues λ of the transition matrix \mathbf{A} (whether real or complex) have an absolute value which is less than 1;

$$\lambda_{\pm} = \frac{a+d}{2} \pm \sqrt{\left(\frac{a+d}{2}\right)^2 - (ad-bc)}. \quad (21)$$

Without contact tracing, there is a chance of epidemic, given the initial reproductive number is $\bar{k} > 1$. In the case of app adoption, the critical value of app-users π_a^c that is needed for reducing the reproductive number can be derived by setting $\lambda = 1$ which leads to:

$$\frac{1 - \pi_a(2 - \pi_{aa})}{1 - \pi_a} \left(\bar{k} + \bar{k}^2 \pi_{aa} (1 - p_{\text{app}}) \right) + \bar{k} \pi_{aa} (1 - p_{\text{app}}) + \frac{\bar{k}^2 \pi_a (1 - \pi_{aa})^2}{1 - \pi_a} = 1. \quad (22)$$

When apps work perfectly, the epidemic threshold is given by:

$$\bar{k}^c = \frac{\sqrt{1 + \pi_a \pi_{aa} [4(\pi_a + \pi_{aa}) - 3(\pi_a \pi_{aa} + 2)]}}{2\pi_a (\pi_{aa} - 1)^2} + \frac{2\pi_a - \pi_a \pi_{aa} - 1}{2\pi_a (\pi_{aa} - 1)^2}. \quad (23)$$

For each value of π_a there is a non-trivial optimum value π_{aa}^{opt} that leads to the largest epidemic threshold in terms of the branching factor, which is:

$$\pi_{aa}^{\text{opt}} = \frac{\pi_a - 2}{3\pi_a - 4}. \quad (24)$$

The critical app adoption can be also calculated as:

$$\pi_a^c = \frac{1 - \bar{k}}{\bar{k}^2(\pi_{aa} - 1)^2 + \bar{k}(\pi_{aa} - 2) + 1}. \quad (25)$$

In the absence of homo/heterophily, $\pi_{aa} = \pi_a$, Eq. 22, gives the same result as of Ref. [41], such that:

$$\pi_a^c = \frac{\bar{k} - 1 + \sqrt{(\bar{k} - 1)(\bar{k} + 3)}}{2\bar{k}}. \quad (26)$$

C. Component size simulations

Next, we describe how to extract the giant component in simulated networks and how these simulation results can be used to find the critical points of the disease spreading process. The component sizes can also be used to find the epidemic size distributions as described in Section IB.

1. Component Extension

In each simulation run, we simulate one network structure G and distribute the apps to the nodes according to one of the models described in Section IC. From the original network G , we keep each link with probability $p = 1 - e^{-\beta\tau}$, which is the probability of infection going through a link without apps. We also remove all the links between two app-users with probability p_{app} and call the resulting network G_a . The components of graph G_a are the normal components.

The extended components can be reached by going through every normal component and extending it. For every app-user in the component $\alpha \in C$, we go through the neighbors $n_\alpha = \{\alpha_1, \alpha_2, \dots, \alpha_k\}$ in the original network G . If α_i is an app-user and not in the component $\alpha_i \notin C$, we add it to the component extension C' with probability p . The total set of infected nodes, if starting from a node in C , will be $C \cup C'$. As these are disjoint sets, we can compute the size as $S'_C = |C| + |C'|$ and $S_c = |C|$.

2. Susceptibility

In numerical simulations of finite size systems, we can use the peak of a susceptibility measure to find the critical transition point. Theoretically, susceptibility [55] is a measure of fluctuation in the component sizes, which is singular at the epidemic threshold (the critical point). In network percolation studies, it is defined as the expected growth in the size of the giant component when a random link is added to the network. Therefore, susceptibility in an ordinary percolation problem can be written as:

$$\chi = \frac{\sum_{c \neq c_{\max}} S_c^2 - S_{c_{\max}}^2}{N - S_{c_{\max}}}, \quad (27)$$

where S_c is the size of the component c , $c_{\max} = \text{argmax}_c S_c$ is the largest component.

This formulation of susceptibility is not suitable in the current case. In fact, using the maximum value of Eq. 27 could lead to estimates of critical points that are very far from the actual one. Instead, we want to compute the expected growth in the extended giant component, which can be computed as:

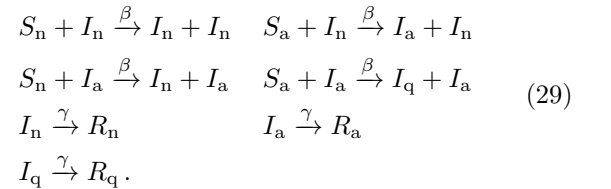
$$\chi' = \frac{\sum_{c \neq c_{\max}} S_c S'_c (1 - \frac{S'_{c_{\max}}}{N})}{N - S_{c_{\max}}}, \quad (28)$$

where S_c and S'_c are the size and the extended size of the component c and $c_{\max} = \text{argmax}_c S'_c$ is the largest component measured in the extended size.

D. Explicit compartment model simulations

Finally, we will perform explicit simulations of the spreading processes to confirm the theoretical results we arrived at via the approximations we presented above. The effect of tracking applications can be integrated into compartment model simulation by introducing separate susceptible and infected compartments for people with and without the app. The interactions between people with no app installed is the same as normal SIR process, namely, susceptible individuals with no app S_n can become infected I_n by being in contact with infected people that either do not have the app installed I_n or have it installed I_a . However, if a susceptible individual with the app S_a comes into contact with an infected individual with app I_a , they will become infected but they will also receive infection notification from the app which means they will be quarantined I_q . Quarantined individuals cannot infect anyone else. Eventually, all the infected individuals will move to the recovered compartment after a certain predetermined amount of time has passed. The recovered compartment is divided into three compartments (R_n , R_a , and R_q) to track from which infected compartment the node is originating from.

The set of all reactions can be written as follows:



Note that, unlike most common SIR models, while edge reactions governed by Poisson processes happening at a constant rate β , node reactions are governed by constant cutoff time $1/\gamma$ and happen exactly $1/\gamma$ units of time after a state change.

As interactions in the simulation are bound to take place over edges of a static network, with nodes belonging to each of the compartments, as shown in Sec. III, the results are similar to a component size simulation (which

are described in Sec. II C) on a network with effective connectivity of $\bar{k} = \langle k \rangle (1 - e^{-\beta/\gamma})$. As it is only the ratio between β and γ that plays as a parameter in the model, we set the value of γ to 1.

In each simulation, starting from a single infected node and running the simulation in discrete time steps of 10^{-4} units until no further reaction is possible, the final number of nodes that end up in R_q , R_a and R_n determine total size of infection corresponding to the extended component size S' of the component that the initial seed node belongs to. The final combined size of the R_n and R_a component, however, represents the size of the component S_n that the seed node belongs to, had we removed app-app links. By adding I_a and I_q compartments, as compared to normal SIR processes, and linking them to the state of the source of infection and the internal state of each node, we include information about the history of the spreading agent more than one step back in the simulation of the spreading process.

III. NUMERICAL RESULTS

We will next illustrate using the theory and simulation introduced in Sec. II how the various parameters affect the epidemic sizes and epidemic probabilities. The simulation studies are done in networks of 10^4 nodes and averaged over 10 realizations. We use two network topologies: homogeneous networks (Erdős-Rényi networks) with expected degree $\langle k \rangle = 10$ and networks created with the configuration model with power-law degree distribution $p(k) \propto k^{-3}$, where the amount of degree 1 nodes is adjusted such that the average degree is 10.

A. Differences in normal and extended components

The difference between the epidemic probability (normal component size) and the epidemic size (extended component size) is a phenomenon specific to epidemics in the presence of app-adaptors. Breaking the equivalence of these two measures can have practical consequences, as illustrated in Fig. 2a. The difference between these two grows with the fraction of app-users π_a . For example, when $\pi_a = 0.8$ and the epidemic probability (the normal component size) is $s_{\max} \approx 0.5$, the epidemic size (the extended component size) reaches $s_{\max} \approx 0.8$. This is also reflected in the expected epidemic sizes (see Fig. 2b). Despite the two component definitions differing from each other, they still display the transition at the same point and this point can be measured numerically using the susceptibilities defined in Eqs. (27)-(28) (see Fig. 2c).

The extended component size is not a conserved quantity like the normal component size in the sense that the sum of component sizes S_{Σ} would always sum to the number of nodes N . Instead, the sum of component sizes can be significantly larger than the number of nodes (see Fig. 2d) and the maximum value it can reach grows with

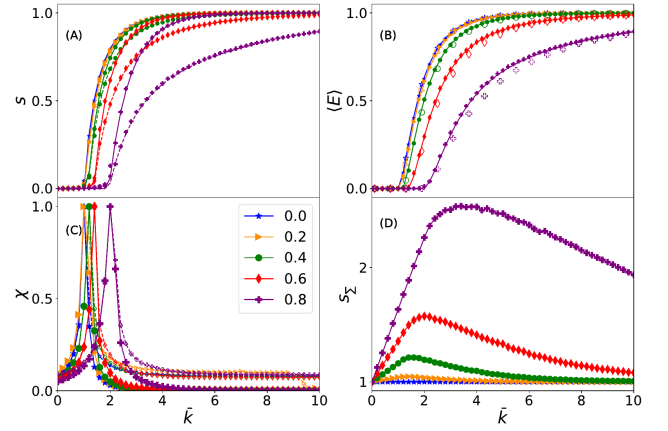


FIG. 2. Disease spreading statistics in an Erdős-Rényi network as a function of the effective degree \bar{k} when there are π_a applications that are distributed uniformly randomly. Results are normalised to the network size N and shown for $\pi_a \in [0, 0.2, 0.4, 0.6, 0.8]$ with different markers. (a) The normal component size, i.e., the epidemic probability (dashed lines and markers following them) and the extended components, i.e., the epidemic size (solid lines and markers following them). Dashed and solid lines indicate the results from theory introduced in Sec. II A and the markers are results computed from component sizes of simulated networks as described in Sec. II C. (b) The expected epidemic size computed with theoretical results introduced in Sec. II A (solid lines), simulated component sizes introduced in Sec. II C (filled markers), and explicit SIR simulations introduced in Sec. II C (empty markers). (c) Susceptibility of the normal giant component χ (dots) and the extended component χ' (solid lines). Peaks are at the same positions for both types of curves. (d) The fraction of sum of component sizes and network size S_{Σ}/N .

the number of application users π_a . The deviation from $S_{\Sigma}/N = 1$ reaches its maximum with disease parameters higher than the threshold values, but when the disease reaches a large enough population, the fraction S_{Σ}/N starts to decay, reaching $S_{\Sigma}/N = 1$ when everybody belongs to the normal giant component.

B. Quarantine failures

The assumption in Section III A is that i) apps work perfectly and ii) an app-user always self-isolates before having a chance to spread the infection, meaning that there are no quarantine failures, $p_{\text{app}} = 1$. It is of practical significance to investigate the effects of quarantine failures [46] on the epidemic threshold and epidemic size. Fig. 3 shows that in the absence of major quarantine failures, epidemic tracing and mitigation with apps can still be a valid strategy if the app adoption level in a society is high enough. The effect of app adoption rate π_a is more important than the rate at which apps function, but both need to be relatively high in order for the apps to have a significant impact.

Even if we are above the epidemic threshold, the apps

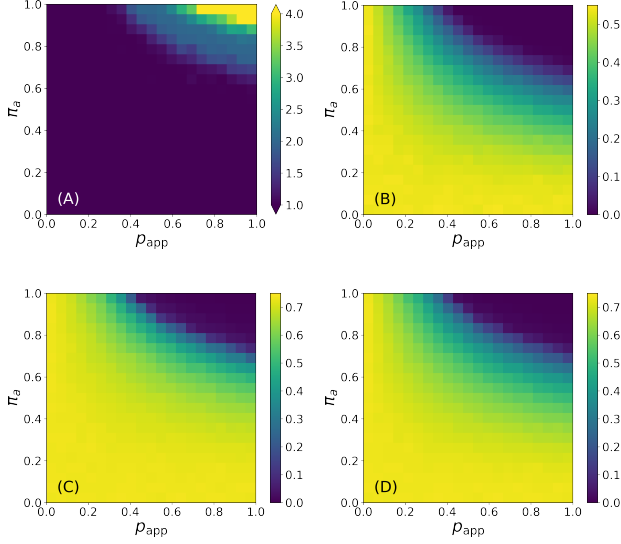


FIG. 3. The effect of quarantine failures in homogeneous networks when app adoption is done uniformly randomly. (a) The epidemic threshold as a function of quarantine probability p_{app} and app adoption rate π_a . All threshold values larger than 4 are shown with the same color. By setting the effective connectivity of the network to $\bar{k} = 1.8$ (b) the expected epidemic size, (c) the extended giant component size and (d) the normal giant component size are shown as a function of p_{app} and π_a .

can be useful. Especially when the application adoption π_a is high, the quarantines can be very unreliable and the outbreak size (Fig. 3b-c) and epidemic probability (Fig. 3d) both remain small. Again, overall, app adoption and quarantine reliability are essential, with the app adoption rate being more important.

C. Degree heterogeneity and high-degree app targeting

Real networks are degree-heterogeneous and this heterogeneity has a strong effect on the final outbreak size and the epidemic threshold. Fig. 4 shows the expected epidemic sizes with two different strategies in app adoption, random and high-degree targeting for different fractions of app-users π_a in the network. In homogeneous networks, Fig. 4a, contact tracing decreases the expected epidemic size and pushes the epidemic threshold forward. These effects can be further amplified by shifting to the high-degree targeting in app adoption. With 80% of app-users, the epidemic threshold can move from $\bar{k} = 1$ to $\bar{k} = 4$, which means at that point expected epidemic size is zero, while without contact tracing it would be almost 1. Note that in homogeneous networks, the effective average degree of the contact network \bar{k} , has good correspondence to the reproduction number of the infection.

In networks with degree-heterogeneity, the epidemic

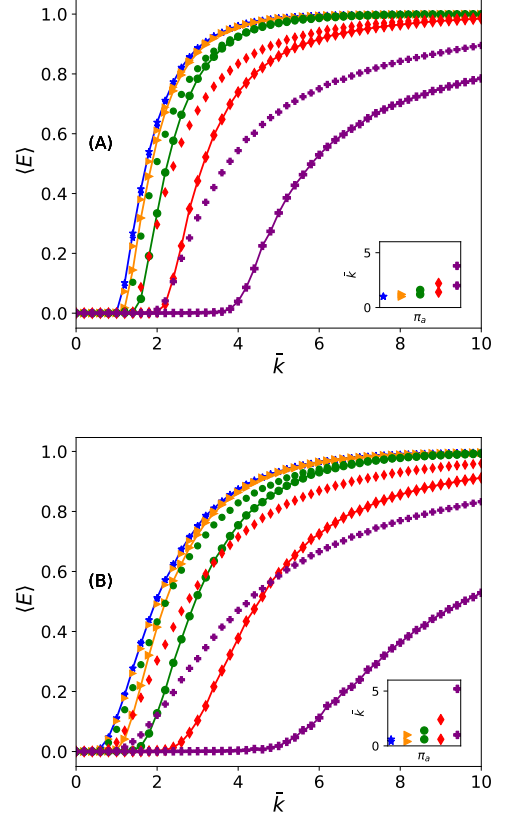


FIG. 4. Expected epidemic size $\langle E \rangle$ as a function of effective degree \bar{k} . Results are shown for different values of π_a using different markers: 0 (stars), 0.2 (triangles), 0.4 (discs), 0.6 (diamonds), and 0.8 (crosses). The solid lines with markers indicate the high-degree targeting strategy, while single markers indicate the random app adoption. The insets show the epidemic threshold for the two strategies as a function of app-adoption rate π_a (such that the upper point is always the high-degree targeting strategy). Results are shown for two network topologies; (a) homogeneous networks with Poisson degree distribution and (b) heterogeneous networks with a power-law degree distribution $P(k) \propto k^{-3}$.

threshold vanishes in normal SIR processes. This effect holds in contact-traced epidemics if we distribute the apps uniformly randomly. However, from Fig. 4b it is clear that contact tracing can significantly reduce the expected epidemic size even when the apps are randomly distributed and the epidemic threshold remains unchanged. With the high-degree targeting strategy, it is possible to move the epidemic threshold. Comparing the expected epidemic size at different values of $\bar{k} < 3$ shows that in real-world situations, app adoption of superspreaders is of significant importance. Since hubs become the app-users, this strategy has drastic effects on the size and threshold of the epidemic, such that the threshold gets pushed from somewhere near zero to a value $\bar{k} > 5$ with the app adoption rate $\pi_a = 0.8$. Therefore, the reproduction number can be much more con-

trolled in the high-degree targeting strategy.

D. The effect of homophily and heterophily

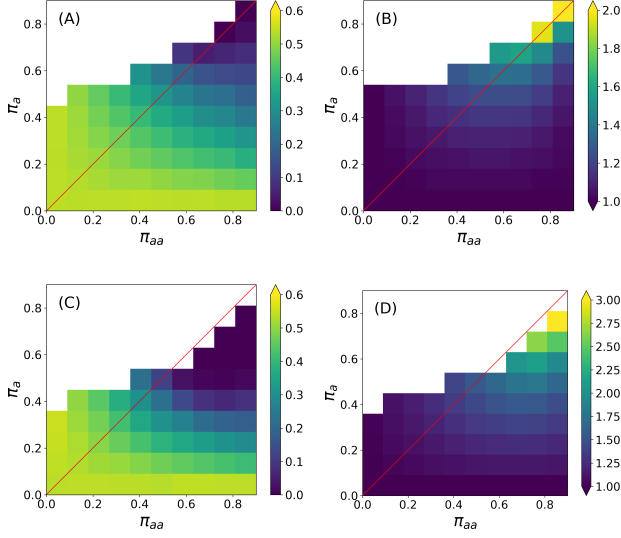


FIG. 5. The effect of homophily/heterophily in app adoption in homogeneous networks. Homophily (heterophily) region is below (above) the diagonal $\pi_a = \pi_{aa}$. Expected epidemic size at $\bar{k} = 1.8$ for (a) random app adoption and for (c) high-degree targeting strategy. Epidemic threshold for (b) random app adoption and for (d) the high-degree targeting strategy. Thresholds are from theoretical results and expected epidemic sizes are from percolation simulations. The empty white region is the spectrum that having such a homo/heterophilic population is impossible.

In previous sections, there was an assumption that app-users are disturbed with random mixing patterns; the fact that one of the connections of a node is an app-user has no effect on the probability of that node being an app adopter. Next, we explore how homophily/heterophily affects the epidemics based on the app usage.

The Fig. 5 illustrates that increasing heterophily leads to a lower epidemic threshold and larger epidemic size for a fixed \bar{k} . Increasing homophily from random mixing is initially preferable, but the optimum lies between random mixing and full homophily. For the expected epidemic size, strong heterophily is especially detrimental (see Fig. 5a for the homogeneous network and with random app adoption and in Fig. 5c for high-degree targeting strategy). The optimum value for heterophily/homophily is evident for the epidemic thresholds in Fig. 5b and Fig. 5d, respectively, for the random and high-degree targeting strategies. Fig. 6b gives a more clear picture of existence of an optimum value for the epidemic threshold in the case of homophily. According to Eq. 23, for each fraction of app-users π_a in the network, the epidemic threshold $\bar{k}^c(\pi_a, \pi_{aa})$ can be maximised by controlling

the homophily in app adoption π_{aa} . The pattern in the Fig. 6b is very similar to the convex pattern in Fig. 5b, even though they are calculated using different approximations and approaches (see Sec. II A and Sec. II B).

Another view on the effect of homophily and heterophily is given by finding the critical fraction app-users π_a^c that is needed to go beyond the epidemic threshold as a function of (π_{aa} and \bar{k}). Fig. 6a depicts this relationship based on Eq. 25 and shows that π_a^c is not monotonic function of π_{aa} but there is an optimal value of π_{aa} giving the lowest fraction apps that are needed to stop the epidemic. Note that in a network without homophily or heterophily π_a^c increases monotonically as the function of the effective connectivity \bar{k} (see the inset of Fig. 6a).

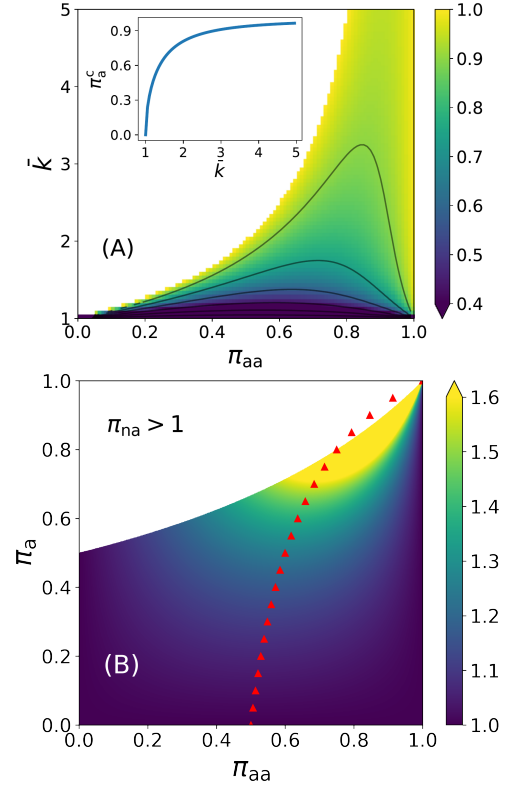


FIG. 6. Existence of optimum value for homophily based on branching process approximation. (a) The critical value of app-users π_a^c that are needed for reducing the reproductive number as a function of effective connectivity and homophily probability π_{aa} . The value of π_a^c remains the same within each black curve. The inset is the graph of π_a^c as a function of \bar{k} in the absence of homophily $\pi_{aa} = \pi_a$ given by Eq. 26. (b) The epidemic threshold \bar{k} as a function of π_{aa} and π_a . The red symbols show the π_{aa}^{opt} for each π_a which is given by to Eq. 24. The pattern here is consistent with another approximation shown in Fig. 5b, while epidemic threshold values are slightly different due to different levels of approximations. Note that here we display the epidemic threshold for all values of π_{aa} and π_a such that $0 \leq \pi_{na} \leq 1$ so the networks with some of these parameters can be created in practice [89].

IV. DISCUSSIONS

In this article, we have developed two flexible analytic approximations to SIR epidemics in the presence of contact tracing apps. First, we use a branching process to derive explicit analytical solutions for the epidemic thresholds. Second, we expand the framework of using consistency equations to analyze digital contact tracing [41], which is an alternative to other approaches [70]. Contrary to the conventional SIR spreading, a full picture of the late-state epidemics in the presence of digital contact tracing is not given by a single observable (the component size), but one also needs two variables (normal and extended component sizes). These correspond to the probability of the epidemic and the epidemic size, which are equivalent in the SIR process. Here we see that the two quantities can be significantly different if the number of application users is high.

Our numerical results illustrate that the effects of digital contact tracing can be very sensitive to the network structure, how applications are distributed among the population, and how well the tracing works. That is, realistic estimates of the effects of digital contact tracing can only be achieved if one is able to choose correct parameter ranges in a high-dimensional parameter space. In this study, we had 6 of such parameters: the shape of the degree distribution, average degree, amount of heterophily/homophily, application prevalence, quarantine probability and targeting strategy. While we were able to establish and confirm basic laws governing individual parameters and some combinations of parameters, exploring such a parameter space fully for possible compound effects is out of the reach in simulations. However, these types of effects can be largely revealed by inspecting the analytic equations we derived.

There are several open questions for which this study and other studies only hint at the results. There are types of network structures we ignore here. For example, the heterophily and homophily could be constructed in the network in slightly different ways. For exam-

ple, a case-study using a realistic agent-based model [54] has recently considered, among many other modelling choices aimed at precise calibration on French population, the contributions of individuals of different ages. One could also develop a more realistic version of our stylized model in order to systematically analyse the effects of homophily caused by an age-based contact structure and different scenarios of app adoption within that structure. The age-based approach would also allow one to estimate the benefits of applications relative to the risk groups in this model.

Overall the problem of digital contact tracing offers not only a practical problem to solve but also an interesting theoretical puzzle because it introduces memory to the epidemic process. This memory is limited to one step within the tracing model we use here, but one could also use multi-step tracing, where also the second neighbors of infected nodes are quarantined in the case that the first neighbors have already passed on the infection. Further, here we ignore effects such as quarantines that do not directly stop the infection from one application user to another from spreading further. However, in the case of a strong group structure in the network, there could be situations where a non-application user A infects application user B, who alerts another application user C, who actually gets infected by A and stops the spreading because of the quarantine. Analyzing such more complicated phenomena can provide challenges for network scientists for years to come.

ACKNOWLEDGEMENT

The simulations presented above were performed using computer resources within the Aalto University School of Science “Science-IT” project. AF acknowledges funding by Science Foundation Ireland Grant No. 16/IA/4470, No. 16/RC/3918, No. 12/RC/2289P2 and No. 18/CRT/6049.

-
- [1] N. Perra, Non-pharmaceutical interventions during the covid-19 pandemic: A review, *Physics Reports* <https://doi.org/10.1016/j.physrep.2021.02.001> (2021).
 - [2] Y. Cheng, N. Ma, C. Witt, S. Rapp, P. S. Wild, M. O. Andreae, U. Pöschl, and H. Su, Face masks effectively limit the probability of sars-cov-2 transmission, *Science* (2021).
 - [3] M. J. Keeling and P. Rohani, *Modeling infectious diseases in humans and animals* (Princeton university press, 2011).
 - [4] W. H. Foege, J. D. Millar, and J. M. Lane, Selective epidemiologic control in smallpox eradication, *American journal of epidemiology* **94**, 311 (1971).
 - [5] K. C. Swanson, C. Altare, C. S. Wesseh, T. Nyenswah, T. Ahmed, N. Eyal, E. L. Hamblion, J. Lessler, D. H. Peters, and M. Altmann, Contact tracing performance during the ebola epidemic in liberia, 2014-2015, *PLoS neglected tropical diseases* **12**, e0006762 (2018).
 - [6] G. W. Rutherford and J. M. Woo, Contact tracing and the control of human immunodeficiency virus infection, *JAMA* **259**, 3609 (1988).
 - [7] G. J. Fox, S. E. Barry, W. J. Britton, and G. B. Marks, Contact investigation for tuberculosis: a systematic review and meta-analysis, *European Respiratory Journal* **41**, 140 (2013).
 - [8] A. Aleta, D. Martin-Corral, A. P. y Piontti, M. Ajelli, M. Litvinova, M. Chinazzi, N. E. Dean, M. E. Halloran, I. M. Longini Jr, S. Merler, *et al.*, Modelling the impact of testing, contact tracing and household quarantine on second waves of covid-19, *Nature Human Behaviour* **4**, 964 (2020).

- [9] P. G. Walker, C. Whittaker, O. J. Watson, M. Baguelin, P. Winskill, A. Hamlet, B. A. Djafaara, Z. Cucunubá, D. O. Mesa, W. Green, *et al.*, The impact of covid-19 and strategies for mitigation and suppression in low-and middle-income countries, *Science* **369**, 413 (2020).
- [10] S. M. Kissler, C. Tedijanto, E. Goldstein, Y. H. Grad, and M. Lipsitch, Projecting the transmission dynamics of sars-cov-2 through the postpandemic period, *Science* **368**, 860 (2020).
- [11] J. Bell, G. Bianconi, D. Butler, J. Crowcroft, P. C. Davies, C. Hicks, H. Kim, I. Z. Kiss, F. Di Lauro, C. Maple, *et al.*, Beyond covid-19: network science and sustainable exit strategies, *Journal of Physics: Complexity* **2**, 021001 (2021).
- [12] M. Gilbert, M. Dewatripont, E. Muraille, J.-P. Platteau, and M. Goldman, Preparing for a responsible lockdown exit strategy, *Nature medicine* **26**, 643 (2020).
- [13] N. E. Kogan, L. Clemente, P. Liautaud, J. Kaashoek, N. B. Link, A. T. Nguyen, F. S. Lu, P. Huybers, B. Resch, C. Havas, A. Petutschnig, J. Davis, M. Chinazzi, B. Mustafa, W. P. Hanage, A. Vespignani, and M. Santillana, An early warning approach to monitor covid-19 activity with multiple digital traces in near real time, *Science Advances* **7**, 10.1126/sciadv.abd6989 (2021).
- [14] S. Kojaku, L. Hébert-Dufresne, E. Mones, S. Lehmann, and Y.-Y. Ahn, The effectiveness of backward contact tracing in networks, *Nature Physics* , 1 (2021).
- [15] M. Salathe, L. Bengtsson, T. J. Bodnar, D. D. Brewer, J. S. Brownstein, C. Buckee, E. M. Campbell, C. Cattuto, S. Khandelwal, P. L. Mabry, *et al.*, Digital epidemiology, *PLoS Comput Biol* **8**, e1002616 (2012).
- [16] A. Natarajan, H.-W. Su, and C. Heneghan, Assessment of physiological signs associated with covid-19 measured using wearable devices, *NPJ digital medicine* **3**, 1 (2020).
- [17] D. R. Seshadri, E. V. Davies, E. R. Harlow, J. J. Hsu, S. C. Knighton, T. A. Walker, J. E. Voos, and C. K. Drummond, Wearable sensors for covid-19: a call to action to harness our digital infrastructure for remote patient monitoring and virtual assessments, *Frontiers in Digital Health* **2**, 8 (2020).
- [18] D. P. Oran and E. J. Topol, Prevalence of asymptomatic sars-cov-2 infection: a narrative review, *Annals of internal medicine* **173**, 362 (2020).
- [19] E. Morales-Narváez and C. Dincer, The impact of biosensing in a pandemic outbreak: Covid-19, *Biosensors and Bioelectronics* **163**, 112274 (2020).
- [20] G. Quer, J. M. Radin, M. Gadaleta, K. Baca-Motes, L. Ariniello, E. Ramos, V. Kheterpal, E. J. Topol, and S. R. Steinhubl, Wearable sensor data and self-reported symptoms for covid-19 detection, *Nature Medicine* **27**, 73 (2021).
- [21] T. Mishra, M. Wang, A. A. Metwally, G. K. Bogu, A. W. Brooks, A. Bahmani, A. Alavi, A. Celli, E. Higgs, O. Dagan-Rosenfeld, *et al.*, Pre-symptomatic detection of covid-19 from smartwatch data, *Nature Biomedical Engineering* **4**, 1208 (2020).
- [22] A. Ganguli, A. Mostafa, J. Berger, M. Y. Aydin, F. Sun, S. A. S. de Ramirez, E. Valera, B. T. Cunningham, W. P. King, and R. Bashir, Rapid isothermal amplification and portable detection system for sars-cov-2, *Proceedings of the National Academy of Sciences* **117**, 22727 (2020).
- [23] P. Fozouni, S. Son, M. D. de León Derby, G. J. Knott, C. N. Gray, M. V. D'Ambrosio, C. Zhao, N. A. Switz, G. R. Kumar, S. I. Stephens, *et al.*, Direct detection of sars-cov-2 using crispr-cas13a and a mobile phone, *MedRxiv* (2020).
- [24] C. Menni, A. Valdes, M. B. Freydin, S. Ganesh, J. E.-S. Moustafa, A. Visconti, P. Hysi, R. C. Bowyer, M. Mangino, M. Falchi, *et al.*, Loss of smell and taste in combination with other symptoms is a strong predictor of covid-19 infection, *MedRxiv* (2020).
- [25] T. Varsavsky, M. S. Graham, L. S. Canas, S. Ganesh, J. C. Pujol, C. H. Sudre, B. Murray, M. Modat, M. J. Cardoso, C. M. Astley, *et al.*, Detecting covid-19 infection hotspots in england using large-scale self-reported data from a mobile application: a prospective, observational study, *The Lancet Public Health* **6**, e21 (2021).
- [26] A. Ganguli, A. Ornob, H. Yu, G. Damhorst, W. Chen, F. Sun, A. Bhuiya, B. Cunningham, and R. Bashir, Hands-free smartphone-based diagnostics for simultaneous detection of zika, chikungunya, and dengue at point-of-care, *Biomedical microdevices* **19**, 1 (2017).
- [27] L. B. Sousa, S. R. Fricker, S. S. Doherty, C. E. Webb, K. L. Baldock, and C. R. Williams, Citizen science and smartphone e-entomology enables low-cost upscaling of mosquito surveillance, *Science of the Total Environment* **704**, 135349 (2020).
- [28] N. G. Becker, K. Glass, Z. Li, and G. K. Aldis, Controlling emerging infectious diseases like sars, *Mathematical biosciences* **193**, 205 (2005).
- [29] M. Eichner, Case isolation and contact tracing can prevent the spread of smallpox, *American journal of epidemiology* **158**, 118 (2003).
- [30] K. T. Eames and M. J. Keeling, Contact tracing and disease control, *Proceedings of the Royal Society of London. Series B: Biological Sciences* **270**, 2565 (2003).
- [31] I. Z. Kiss, D. M. Green, and R. R. Kao, Infectious disease control using contact tracing in random and scale-free networks, *Journal of The Royal Society Interface* **3**, 55 (2006).
- [32] R. M. HOWELL, W. J. Kassler, and A. Haddix, Partner notification to prevent pelvic inflammatory disease in women: cost-effectiveness of two strategies, *Sexually transmitted diseases* **24**, 287 (1997).
- [33] C. Fraser, S. Riley, R. M. Anderson, and N. M. Ferguson, Factors that make an infectious disease outbreak controllable, *Proceedings of the National Academy of Sciences* **101**, 6146 (2004).
- [34] M. Kretzschmar, Y. T. van Duynhoven, and A. J. Severijnen, Modeling prevention strategies for gonorrhea and chlamydia using stochastic network simulations, *American Journal of Epidemiology* **144**, 306 (1996).
- [35] D. Klinkenberg, C. Fraser, and H. Heesterbeek, The effectiveness of contact tracing in emerging epidemics, *PloS one* **1**, e12 (2006).
- [36] R. Huerta and L. S. Tsimring, Contact tracing and epidemics control in social networks, *Phys. Rev. E* **66**, 056115 (2002).
- [37] P. Rodríguez, S. Graña, E. E. Alvarez-León, M. Battaglini, F. J. Darias, M. A. Hernán, R. López, P. Llana, M. C. Martín, O. Ramirez-Rubio, *et al.*, A population-based controlled experiment assessing the epidemiological impact of digital contact tracing, *Nature communications* **12**, 1 (2021).
- [38] I. Braithwaite, T. Callender, M. Bullock, and R. W. Aldridge, Automated and partly automated contact tracing: a systematic review to inform the control of covid-19,

- The Lancet Digital Health (2020).
- [39] M. Salathé, C. L. Althaus, N. Anderegg, D. Antonioli, T. Ballouz, E. Bugnion, S. Capkun, D. Jackson, S.-I. Kim, J. Larus, *et al.*, Early evidence of effectiveness of digital contact tracing for sars-cov-2 in switzerland, medRxiv (2020).
 - [40] J. O’Connell and D. T. O’Keeffe, Contact tracing for covid-19—a digital inoculation against future pandemics, New England Journal of Medicine (2021).
 - [41] A. Barrat, C. Cattuto, M. Kivelä, S. Lehmann, and J. Saramäki, Effect of manual and digital contact tracing on covid-19 outbreaks: a study on empirical contact data, medRxiv 10.1101/2020.07.24.20159947 (2020).
 - [42] E. Shim, A. Tariq, W. Choi, Y. Lee, and G. Chowell, Transmission potential and severity of covid-19 in south korea, International Journal of Infectious Diseases **93**, 339 (2020).
 - [43] J. Cohen and K. Kupferschmidt, Countries test tactics in ‘war’ against covid-19 (2020).
 - [44] G. Cencetti, G. Santin, A. Longa, E. Pigani, A. Barrat, C. Cattuto, S. Lehmann, M. Salathe, and B. Lepri, Digital proximity tracing on empirical contact networks for pandemic control, medRxiv, 2020 (2021).
 - [45] H. L. Hambridge, R. Kahn, and J.-P. Onnela, Examining sars-cov-2 interventions in residential colleges using an empirical network, medRxiv 10.1101/2021.03.09.21253198 (2021).
 - [46] C. Wymant, L. Ferretti, D. Tsallis, M. Charalambides, L. Abeler-Dörner, D. Bonsall, R. Hinch, M. Kendall, L. Milsom, M. Ayres, *et al.*, The epidemiological impact of the nhs covid-19 app, Alan Turing Institute: London, UK (2021).
 - [47] R. Pastor-Satorras and A. Vespignani, *Evolution and structure of the Internet: A statistical physics approach* (Cambridge University Press, 2007).
 - [48] S. N. Dorogovtsev and J. F. Mendes, *Evolution of networks: From biological nets to the Internet and WWW* (OUP Oxford, 2013).
 - [49] R. Albert and A.-L. Barabási, Statistical mechanics of complex networks, Reviews of modern physics **74**, 47 (2002).
 - [50] R. Pastor-Satorras and A. Vespignani, Epidemic spreading in scale-free networks, Physical review letters **86**, 3200 (2001).
 - [51] D. Centola, An experimental study of homophily in the adoption of health behavior, Science **334**, 1269 (2011).
 - [52] S. Funk, M. Salathé, and V. A. Jansen, Modelling the influence of human behaviour on the spread of infectious diseases: a review, Journal of the Royal Society Interface **7**, 1247 (2010).
 - [53] V. von Wyl, M. Höglinger, C. Sieber, M. Kaufmann, A. Moser, M. Serra-Burriel, T. Ballouz, D. Menges, A. Frei, and M. A. Puhon, Drivers of acceptance of covid-19 proximity tracing apps in switzerland: panel survey analysis, JMIR public health and surveillance **7**, e25701 (2021).
 - [54] J. A. M. López, B. A. García, P. Bentkowski, L. Bioglio, F. Pinotti, P.-Y. Boëlle, A. Barrat, V. Colizza, and C. Poletto, Anatomy of digital contact tracing: role of age, transmission setting, adoption and case detection, Science Advances, eabd8750 (2021).
 - [55] M. Newman, *Networks* (Oxford university press, 2018).
 - [56] L. Hébert-Dufresne, B. M. Althouse, S. V. Scarpino, and A. Allard, Beyond r_0 : heterogeneity in secondary infections and probabilistic epidemic forecasting, Journal of the Royal Society Interface **17**, 20200393 (2020).
 - [57] M. Boguná, R. Pastor-Satorras, and A. Vespignani, Absence of epidemic threshold in scale-free networks with degree correlations, Physical review letters **90**, 028701 (2003).
 - [58] M. Barthélemy, A. Barrat, R. Pastor-Satorras, and A. Vespignani, Velocity and hierarchical spread of epidemic outbreaks in scale-free networks, Physical review letters **92**, 178701 (2004).
 - [59] R. Pastor-Satorras and A. Vespignani, Epidemic dynamics in finite size scale-free networks, Physical Review E **65**, 035108 (2002).
 - [60] S. Dhara, R. van der Hofstad, and J. S. van Leeuwen, Critical percolation on scale-free random graphs: new universality class for the configuration model, Communications in Mathematical Physics, 1 (2021).
 - [61] L. Ferretti, C. Wymant, M. Kendall, L. Zhao, A. Nurtay, L. Abeler-Dörner, M. Parker, D. Bonsall, and C. Fraser, Quantifying sars-cov-2 transmission suggests epidemic control with digital contact tracing, Science **368** (2020).
 - [62] P. Sapiezynski, J. Pruessing, and V. Sekara, The fallibility of contact-tracing apps, arXiv preprint arXiv:2005.11297 (2020).
 - [63] Y. Liu, R. M. Eggo, and A. J. Kucharski, Secondary attack rate and superspreading events for sars-cov-2, The Lancet **395**, e47 (2020).
 - [64] Z. Shen, F. Ning, W. Zhou, X. He, C. Lin, D. P. Chin, Z. Zhu, and A. Schuchat, Superspreading sars events, beijing, 2003, Emerging infectious diseases **10**, 256 (2004).
 - [65] S. Cléménçon, H. De Arazoza, F. Rossi, and V. C. Tran, A statistical network analysis of the hiv/aids epidemics in cuba, Social Network Analysis and Mining **5**, 1 (2015).
 - [66] J. O. Lloyd-Smith, S. J. Schreiber, P. E. Kopp, and W. M. Getz, Superspreading and the effect of individual variation on disease emergence, Nature **438**, 355 (2005).
 - [67] K. Kupferschmidt, Why do some covid-19 patients infect many others, whereas most don’t spread the virus at all, Science **10** (2020).
 - [68] S. L. Feld, Why your friends have more friends than you do, American Journal of Sociology **96**, 1464 (1991).
 - [69] M. E. Newman, Threshold effects for two pathogens spreading on a network, Physical review letters **95**, 108701 (2005).
 - [70] G. Bianconi, H. Sun, G. Rapisardi, and A. Arenas, Message-passing approach to epidemic tracing and mitigation with apps, Physical Review Research **3**, L012014 (2021).
 - [71] I. Kryven and C. Stegehuis, Contact tracing in configuration models, Journal of Physics: Complexity **2**, 025004 (2021).
 - [72] A. Allard, C. Moore, S. V. Scarpino, B. M. Althouse, and L. Hébert-Dufresne, The role of directionality, heterogeneity and correlations in epidemic risk and spread, arXiv:2005.11283 (2020).
 - [73] R. B. Simões, I. Amaral, and S. Santos, Tracking the outbreak and far beyond: How are public authorities using mobile apps to control covid-19 pandemic, Multidisciplinary Perspectives of Communication in a Pandemic Context **1**, 166 (2021).
 - [74] M. Abueg, R. Hinch, N. Wu, L. Liu, W. J. Probert, A. Wu, P. Eastham, Y. Shafi, M. Rosencrantz, M. Dikovskiy, *et al.*, Modeling the combined effect of digital exposure notification and non-pharmaceutical inter-

ventions on the covid-19 epidemic in washington state, medRxiv (2020).

- [75] A. Bassolas, A. Santoro, S. Sousa, S. Rognone, and V. Nicosia, Optimising the mitigation of epidemic spreading through targeted adoption of contact tracing apps, arXiv:2102.13013 (2021).
- [76] M. Kendall, L. Milsom, L. Abeler-Dörner, C. Wymant, L. Ferretti, M. Briers, C. Holmes, D. Bonsall, J. Abeler, and C. Fraser, Epidemiological changes on the isle of wight after the launch of the nhs test and trace programme: a preliminary analysis, *The Lancet Digital Health* **2**, e658 (2020).
- [77] G. Burgio, B. Steinegger, G. Rapisardi, and A. Arenas, The impact of homophily on digital proximity tracing, arXiv:2103.00635 (2021).
- [78] M. E. Newman, Spread of epidemic disease on networks, *Physical review E* **66**, 016128 (2002).
- [79] R. Pastor-Satorras, C. Castellano, P. Van Mieghem, and A. Vespignani, Epidemic processes in complex networks, *Reviews of modern physics* **87**, 925 (2015).
- [80] R. Albert, H. Jeong, and A.-L. Barabási, Error and attack tolerance of complex networks, *nature* **406**, 378 (2000).
- [81] R. Cohen, K. Erez, D. Ben-Avraham, and S. Havlin, Resilience of the internet to random breakdowns, *Physical review letters* **85**, 4626 (2000).
- [82] A. Barrat, M. Barthélemy, and A. Vespignani, *Dynamical processes on complex networks* (Cambridge university press, 2008).
- [83] S. N. Dorogovtsev, A. V. Goltsev, and J. F. Mendes, Critical phenomena in complex networks, *Reviews of Modern Physics* **80**, 1275 (2008).
- [84] L. Basnarkov, M. Mirchev, and L. Kocarev, Random walk with memory on complex networks, *Physical Review E* **102**, 042315 (2020).
- [85] P. Shu, Effects of memory on information spreading in complex networks, in *2014 IEEE 17th International Conference on Computational Science and Engineering* (IEEE, 2014) pp. 554–556.
- [86] E. Kenah and J. M. Robins, Second look at the spread of epidemics on networks, *Physical Review E* **76**, 036113 (2007).
- [87] E. Kenah and J. C. Miller, Epidemic percolation networks, epidemic outcomes, and interventions, *Interdisciplinary perspectives on infectious diseases* **2011** (2011).
- [88] B. Bollobás and B. Béla, *Random graphs*, 73 (Cambridge university press, 2001).
- [89] J. P. Gleeson, Cascades on correlated and modular random networks, *Phys. Rev. E* **77**, 046117 (2008).

APPENDIX

About quarantine failures, as it was shown in Fig. 3, Fig. 7 and 8 also show that contact tracing can yield very good results in terms of reducing the epidemic threshold and expected epidemic size if everything goes right at least for 50% and half of the people use the apps. This effect is more prominent if we go for the high-degree targeting strategy, especially in heterogeneous networks, as shown in Fig. 7d and 8d. Fig. 9 and 10 show that there is an optimum value for homophily in app adoption as it

was shown in Fig. 5 and Fig. 6. The only exception is when we follow a high-degree targeting strategy in heterogeneous networks. In this case, we can see the hub effect on the epidemic threshold and size.

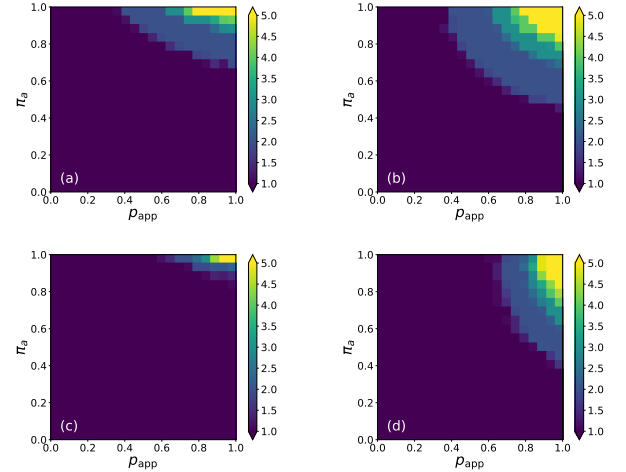


FIG. 7. The epidemic threshold as a function of quarantine probability p_{app} and app adoption rate π_a . The effect of quarantine failures in homogeneous networks with (a) random app adoption (b) and high-degree targeting strategy. Also, for heterogeneous networks with a power-law degree distribution with (c) random app adoption (d) and high-degree targeting strategy. All threshold values larger than 5 are shown with the same color.

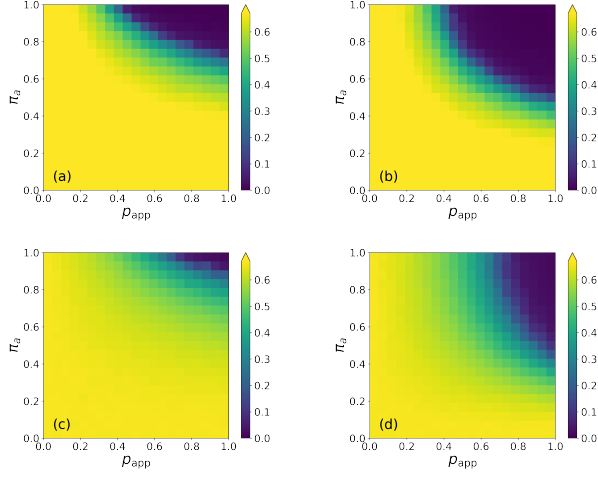


FIG. 8. Expected epidemic size in the case of quarantine failures. Expected epidemic size at $\bar{k} = 1.8$ for homogeneous networks with (a) random app adoption (b) and high-degree targeting strategy. Also, for heterogeneous networks with a power-law degree distribution with (c) random app adoption (d) and high-degree targeting strategy. In (b) and (d) the pattern is different due to the effects of hubs. When doing a high-degree targeting strategy, quarantine failures are more significant since the infected ones are highly influential on the spreading dynamics.

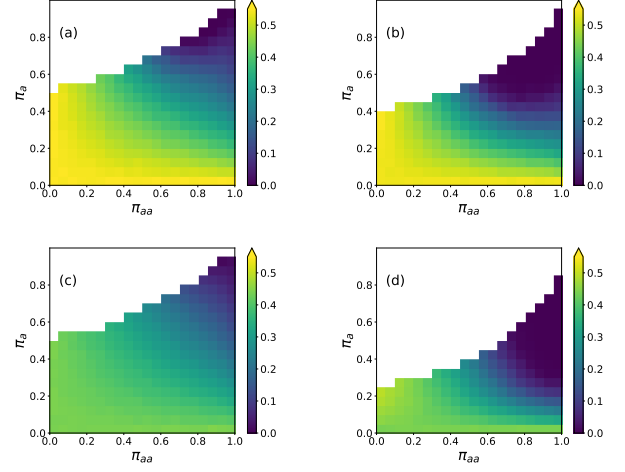


FIG. 9. The effect of homophily/heterophily in app adoption on the expected epidemic size. Expected epidemic size at $\bar{k} = 1.8$ from percolation simulations for homogeneous networks with (a) random app adoption (b) and high-degree targeting strategy. Also, for heterogeneous networks with a power-law degree distribution with (c) random app adoption (d) and high-degree targeting strategy. The empty white region is the spectrum that having such a homo/heterophilic population is impossible.

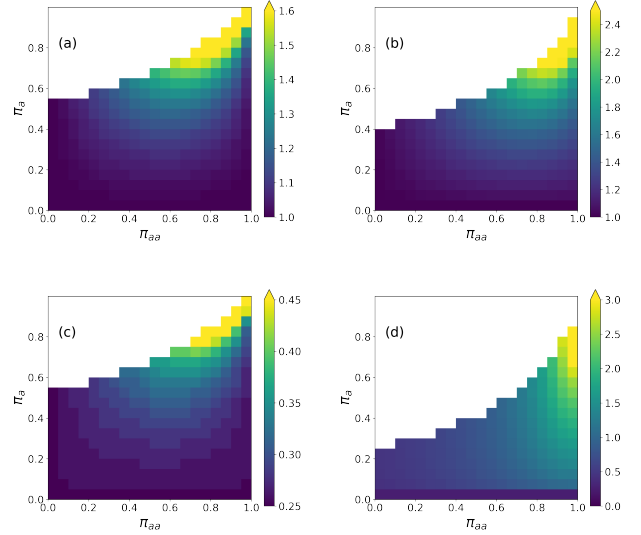


FIG. 10. The effect of homophily/heterophily in app adoption on the epidemic threshold and optimum pattern for homophily. Epidemic thresholds for homogeneous networks with (a) random app adoption (b) and high-degree targeting strategy. Also, for heterogeneous networks with a power-law degree distribution with (c) random app adoption (d) and high-degree targeting strategy. The empty white region is the spectrum that having such a homo/heterophilic population is impossible.